

TRIEX-II: An experimental facility for the characterization of the Tritium Extraction Unit of the WCLL blanket of ITER and DEMO fusion reactors

Original

TRIEX-II: An experimental facility for the characterization of the Tritium Extraction Unit of the WCLL blanket of ITER and DEMO fusion reactors / Uili, Marco; Alberghi, Ciro; Candido, Luigi; Papa, Francesca; Tarantino, Mariano; Venturini, Alessandro. - In: NUCLEAR FUSION. - ISSN 0029-5515. - ELETTRONICO. - 62:6(2022). [10.1088/1741-4326/ac5c74]

Availability:

This version is available at: 11583/2959685 since: 2022-05-11T10:27:01Z

Publisher:

IOP

Published

DOI:10.1088/1741-4326/ac5c74

Terms of use:

This article is made available under terms and conditions as specified in the corresponding bibliographic description in the repository

Publisher copyright

IOP postprint/Author's Accepted Manuscript

"This is the accepted manuscript version of an article accepted for publication in NUCLEAR FUSION. IOP Publishing Ltd is not responsible for any errors or omissions in this version of the manuscript or any version derived from it. The Version of Record is available online at <http://dx.doi.org/10.1088/1741-4326/ac5c74>

(Article begins on next page)

TRIEX-II: An Experimental Facility for the Characterization of the Tritium Extraction Unit of the WCLL Blanket of ITER and DEMO Fusion Reactors

Marco Utili^a, Ciro Alberghi^b, Luigi Candido^b, Francesca Papa^c, Mariano Tarantino^a and Alessandro Venturini^a

^aENEA C.R. Brasimone – Località Brasimone, 40043 Camugnano (BO), Italy

^bESSENTIAL Group, Politecnico di Torino - Corso Duca degli Abruzzi, 24, 10129, Torino, Italy

^cSapienza University of Rome, Department of Astronautical, Electrical and Energy Engineering, Nuclear Section, Corso Vittorio Emanuele II 244, 00186 Roma, Italy

E-mail: marco.utili@enea.it

August 2021

Abstract. The experimental qualification of the Tritium Extraction Unit (TEU) from the LiPb eutectic alloy (15.7 at. % Li), the breeder material of the Water-Cooled Lithium-Lead (WCLL) breeding blanket concept, is one of the fundamental items for the demonstration of tritium balance sustainability for ITER and DEMO fusion reactors. Several technologies have been proposed as TEU, but the selection of the reference technology can be carried out only after the experimental measurement of the tritium extraction efficiency. For this purpose, a dedicated facility, called TRIEX-II, was designed and installed at ENEA Brasimone research centre, Italy. The facility is able to qualify Gas-Liquid Contactor (GLC), Permeator Against Vacuum (PAV) and Liquid-Vacuum Contactor (LVC) technologies at different temperatures, lithium-lead mass flow rates and hydrogen isotopes concentrations. In TRIEX-II, the hydrogen or deuterium, used to simulate tritium, are solubilised inside the LiPb with a dedicated saturator and are then extracted from the liquid metal in the GLC mock-up, which uses pure helium or a mixture constituted by helium and hydrogen as stripping gas and works in the temperature range between 300 and 500 °C.

Keywords: TRIEX-II, Tritium Extraction System, Gas-Liquid Contactor, Permeation Against Vacuum, Liquid-Vacuum Contactor. Submitted to: *Nucl. Fusion*

1. Introduction

The Water-Cooled Lithium-Lead (WCLL) concept is under development as Test Blanket System (TBS) [1] for ITER and as candidate driver blanket for DEMO [2]. One of the greatest challenges for the success of the liquid metal breeder concepts is the extraction of tritium from the liquid LiPb eutectic alloy (15.7 at. %Li), which fulfills the functions of tritium breeder, tritium carrier and neutron multiplier [3]. Therefore, the design and characterization of the Tritium Extraction Unit (TEU) is one of the fundamental objectives of the F4E and EUROfusion research efforts. Among the different technologies proposed [4, 5], the Gas-Liquid Contactor (GLC), the Permeator Against Vacuum (PAV) and the Liquid-Vacuum Contactor (LVC) are the prioritized European candidates. The GLC will be used in the ITER TBM programme [6].

In the Gas-Liquid Contactor the LiPb and a stripping gas are brought into contact allowing a diffusion interchange between them. Helium is commonly considered a good choice as stripping gas, with the possibility to add a small percentage of hydrogen to allow the isotopic exchange with tritium [7]. The PAV technology is based on the phenomenon of tritium permeation through a membrane towards a secondary side where vacuum is pumped. In this way, a pressure gradient is established promoting tritium extraction [8]. Finally, in the LVC the liquid metal flows from an upper chamber to a bottom vacuumed one; these chambers are separated by a tray equipped with nozzles of diameter of the order of the millimetre, which allows the alloy to form an unstable liquid jet of droplets. The high theoretical efficiency is due to a continuous evolution of droplets [9]. These three technologies are currently considered good candidates for the TEU, but the final selection is prevented by remarkable uncertainties, such as on the manufacturing techniques and on certain transport properties [10] (e.g. the Sieverts' constant of hydrogen isotopes solubilized into LiPb or the mass transfer coefficient between liquid phase and gas phase). For this reason, an extensive R&D programme was put in place with the aim of providing experimental results of mock-ups of the technologies. In this context, the experimental facility TRIEX-II (Tritium Extraction) was manufactured and installed in ENEA Brasimone research centre, Italy. The currently installed mock-up is the GLC, with the possibility to replace the test section with PAV technology or even with LVC.

The work provides an overview of the facility, focusing on its subsystems, on the main components of the LiPb loop and on the main instruments of the facility. Moreover, a fluid-dynamic characterization is provided, along with the different methods to evaluate

the hydrogen isotopes extraction efficiency of the GLC mock-up.

2. Motivations to the upgrade

In 2007, TRIEX facility [11, 12] was completed with three hydrogen permeation sensors used to measure tritium concentration in LiPb, qualified in a dedicated device. TRIEX had a ring design, chosen so that only the pressure drops had to be overcome. The main components were the recirculation tank S1, the liquid metal pump, the instrumentation, the hydrogen saturator S2, the extractor S3 that adopts a segmented (modular) philosophy, with a filler consisting of waved steel sheets that was objective of the tests to be carried out in the TRIEX facility. The saturator allows the alloy to reach the desired hydrogen concentration. The lead-lithium that comes out from the saturator goes in the Extractor S3 where the packed column is placed. Two sensors were installed in the outlet gas line of saturator and extractor in order to relieve the hydrogen concentration. The range of hydrogen concentration that they have to measure is of the order of 100 ppm. The hydrogen concentration in the liquid metal is measured before the saturator (HLM01), before and after the extractor (HLM02 and HLM03). The synoptic of TRIEX is displayed in Figure 1 [11].

The first test was carried out in 2007 without results due to the failure of the mechanical pump. In 2010, the mechanical pump was re-qualified and inserted in TRIEX loop. The first experimental qualification of Gas-Liquid Contactor used as TEU for the Helium-Cooled Lithium-Lead (HCLL) TBM was completed in 2014. The main drawbacks of the past experimental campaign are reported as follows:

- (i) It was not possible to check the closure of the hydrogen mass balance during the extraction phase due to low accuracy of the instrumentation used to measure the hydrogen concentration (%) at the outlet of the extraction column and of the saturator. The instrumentation was able to relieve the hydrogen concentration (%) at the outlet of the extraction column and of the saturator only for high hydrogen concentration. The range was of the order of 500-5000 ppm instead the hydrogen concentration expected is in the range 10-500 ppm;
- (ii) Only in few cases, it was obtained the evidence of the reached equilibrium between gas and liquid metal phases before starting the extraction phase due to huge response time requested by the hydrogen permeation sensors in LiPb and impossibility of the saturator to replace all hydrogen extracted and permeated through TRIEX walls;

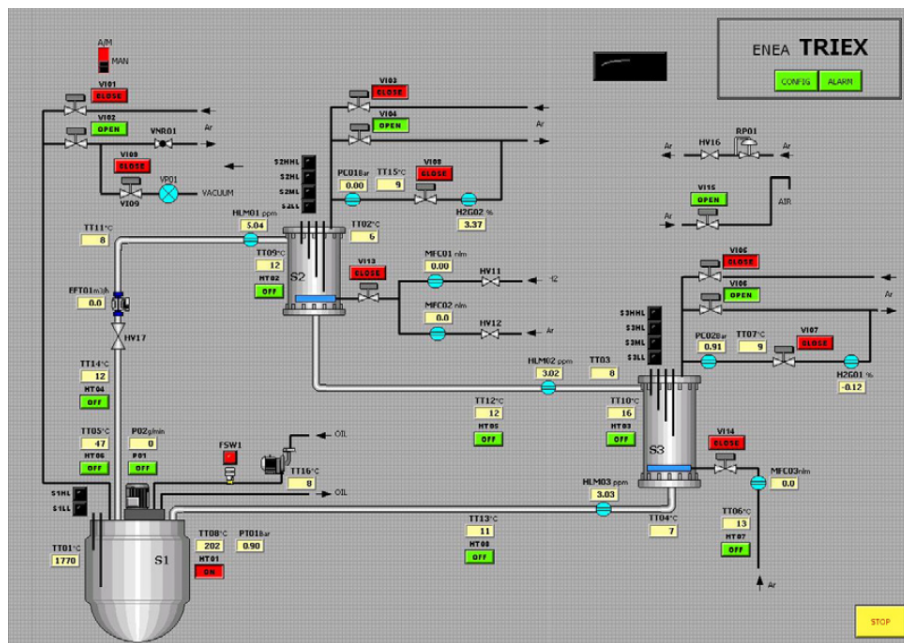


Figure 1: Main window of the DACS of TRIEX facility in 2007.

(iii) A clear trend between extraction efficiency and L/G ratio (ratio between the liquid metal and gas flow-rate), was not found due to the low number of experiments performed.

To increase the efficiency of the saturator and the instrumentation performances, to increase the reliability of the facility (management of the mass flow rate sent to TEU), and to use hydrogen sensor in gas phase able to measure hydrogen isotopes concentration in the range 0.01%-0.5%, it was necessary to perform an upgrade of the facility.

3. Relevance to ITER and DEMO

The main objective to be reached in TRIEX-II facility is to verify the efficiency of the tritium extraction unit in operating conditions relevant for the WCLL Test Blanket System of ITER and for the WCLL Breeding Blanket of DEMO. In particular, TRIEX-II is characterized by the following operating conditions:

- Temperature range of LiPb: 350-500 °C;
- LiPb mass flow rate: 0.2-4.5 kg s⁻¹;
- Gas stripping flow rate: 50-450 NI h⁻¹;
- Maximum Q2 concentration in gas stripping flow rate (saturator): 5%;
- Q partial pressure in LiPb: 10-1000 Pa.

The design parameters of TRIEX-II allow to characterise the GLC technology, which is the priority among the objectives of the facility at relevant TBS

operative conditions. If for ITER the GLC mock-up installed in TRIEX-II can be considered as 1:1 scale, for DEMO allows to investigate the performance of the candidate tritium extraction technologies (GLC and PAV) with the support of a dedicated mock-up in order to support the TER system selection for DEMO.

4. TRIEX-II facility description

TRIEX-II (Figure 2) is a facility designed to characterize the different technologies candidate as the TEU of ITER and DEMO reactors. In particular, the facility will test two kinds of extractor mock-ups: the Gas-Liquid Contactor, in the packed column configuration, and the Permeator Against Vacuum. The aim is to qualify the extraction of hydrogen or deuterium from flowing LiPb in the range of operative conditions foreseen for the WCLL TBM or Breeding Blanket. It is operated with hydrogen (or deuterium) instead of tritium for safety reasons and is equipped with prototypical components customized for LiPb applications. TRIEX-II is manufactured with 2 1/4 Cr-1 Mo steel (ASTM A335 Gr. P22), whose relatively low corrosion rate (low nickel content and consequent low degradation by dissolution [13]) allows the facility to be operated at high temperature for several thousand hours.

Four main systems can be identified:

- (i) the LiPb loop (primary loop);
- (ii) the vacuum system;
- (iii) the gas loop;

(iv) the compressed air circuit.

In the following paragraphs, a description of the different systems is provided.



Figure 2: TRIEX-II LiPb facility.

4.1. LiPb loop

The LiPb loop (Figure 3) consists of the following main components:

- the extractor (GLC mock-up) S300;
- the saturator S200;
- the storage tank S100;
- the permanent magnets pump EP100.

Figure 4 shows the main window of the DACS (Data Acquisition and Control System) of TRIEX-II. The LiPb is stored in the cylindrical storage tank (S100), which is connected through a 1/2" pipe to the rest of the loop. After the loading, the LiPb flows clockwise from the permanent magnets pump (EP100) to the saturator (S200), where hydrogen (or deuterium), carried by a flow of helium, is solubilized in the eutectic liquid metal. The LiPb enters the saturator from the top and exits from the bottom. Then, it flows towards to the top of the extractor (S300), where the mock-up for tritium extraction to be tested is placed.

A thermal mass flow meter is installed between the saturator and the extractor. This instrument was designed by ENEA and Thermocoax and it was characterized in IELLLO facility [14]. The LiPb goes out from the bottom of the extractor and goes back to the pump. A bypass proportional valve is installed upstream of the extractor, with the aim to allow the draining of the pipe between the saturator and the extractor itself. This valve also allows, together with

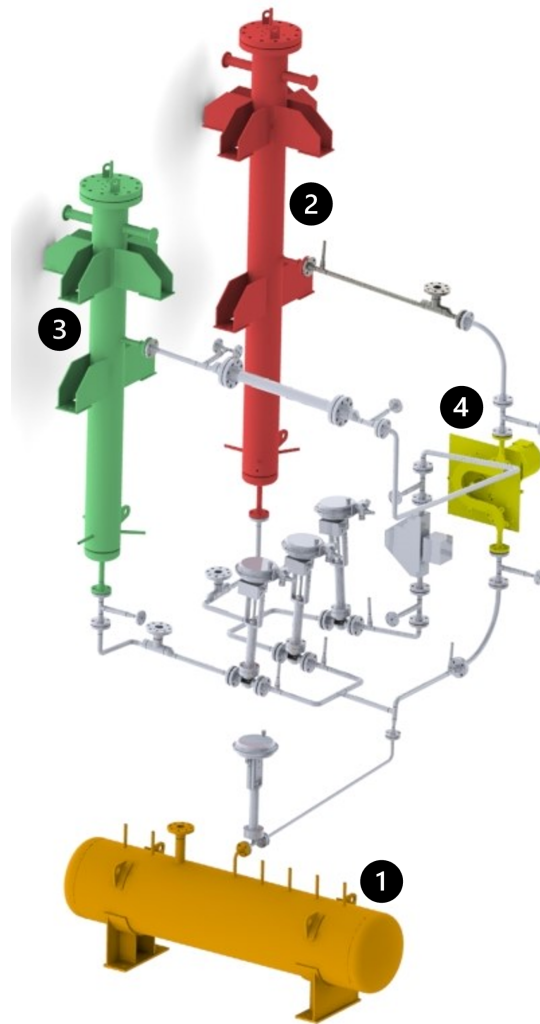


Figure 3: LiPb loop in TRIEX-II. 1: storage tank S100; 2: saturator S200; 3: extractor S300 (GLC mock-up); 4: permanent magnets pump EP100.

the pump, to control the flow rate (measured by the mass flow meter) entering the extractor.

Six internal thermocouples in the LiPb and more than thirty external thermocouples are installed throughout the piping. Each flange of the loop has a leakage detector that warns in case a LiPb leakage happens. Three hydrogen isotopes permeation sensors are used to measure hydrogen concentration in LiPb. These sensors are installed in dedicated chambers located at the inlet of the saturator, between saturator and extractor and at the outlet from the extractor.

The whole loop is heated by means of heating cables or bands and thermally insulated. Each heater is equipped with a control and a safety thermocouple (the control thermocouple monitors the heating rate, while the safety one measures the temperature of the heater, preventing its overheating). The storage tank is equipped with:

- two internal thermocouples at different depths;
- a relative pressure transducer;
- a guided micro-wave level meter;
- three heating bands.

The saturator and the extractor are equipped with:

- two internal thermocouples at different depths;
- three heating bands;
- a relative pressure transducer;
- four discrete level detectors (thermocouples used as electrodes).

4.2. Vacuum system

The vacuum system is divided into two subsystems. The first one uses a rotary vane pump to make vacuum in the LiPb loop. This system is necessary to remove any trace of oxygen before heating up the loop. Then, after 24 hours at 150°C, vacuum is pumped again to remove the impurities that were desorbed by the pipe walls. Finally, the LiPb loading is performed under vacuum to allow the complete filling of the chambers of the helical sensors, which otherwise would remain partially filled by gas.

The second subsystem uses an integrated pumping station, composed of a diaphragm and a turbomolecular pump, to evacuate the hydrogen isotopes permeation sensors, described in detail in Chapter 4.1. Each sensor is connected to the vacuum station by a 1/4" Swagelok line, on which a vacuum pressure transducer and a pneumatic valve are installed. The valve is used to isolate the sensor from the rest of the line during the measurements.

4.3. Gas and compressed air loops

The gas loop connects the gas cylinders (helium and helium + deuterium) and the hydrogen generator to the saturator and to the extractor. The gas stream is used to saturate LiPb in the saturator and as stripping gas in the extractor, when the Gas-Liquid Contactor mock-up is under testing. Each gas line is equipped with a relative pressure transducer, two valves and a mass flow controller. The mass flow controllers are used to mix desired flow rates of hydrogen (or deuterium) and helium. The inlet gas composition is analyzed by a mass spectrometer. The gas leaving the saturator and the extractor is brought to the mass spectrometer by other lines belonging to the gas loop, so that also the outlet gas composition can be measured. Each outlet line is equipped with a mass flow meter.

Finally, the compressed air loop supplies the pneumatic valves and the cooling system of the permanent magnets pump used to circulate the LiPb.

5. Main components

The main components of TRIEX-II facility are described in the following paragraphs.

5.1. Extractor (S300)

The current extractor of TRIEX-II is a mock-up of the Gas-Liquid Contactor. GLC is a well-known industrial technology [15] and already used in experimental qualifications with LiPb [16, 17], even if in these cases the H₂ mass balance was not verified. In this technology, a gas and a liquid are brought into contact, allowing a diffusion exchange between them. The GLC of TRIEX-II is of the packed column type [12]. The packed columns are vertical columns filled with a packing which breaks the liquid flow and provides a large interfacial area between the liquid and the gas phases.

In the packed column, the extraction of the hydrogen isotopes from LiPb is mediated by the use of a stripping gas (helium). The gas injection system is positioned at the bottom of the tank to achieve a complete dispersion of gas bubbles inside the tank containing the LiPb, counter-current with the liquid metal. The continuously injected gas in the tank leaves from the top with appropriate flow control so as to adjust the pressure inside the tank and consequently the level of the LiPb. The packed column can also be lengthened or shortened in order to collect an opportune data set for modelling, varying both the LiPb mass flow rate and the volumetric flow rate of the purge gas. As far as packings are concerned, two main groups can be individuated: the random packing and the structured packing [15]. Structured packing was chosen because of:

- maximisation of the specific surface area, which increases the gas-liquid contact area;
- uniformly spreading of the surface area, augmenting the gas-liquid contact;
- maximisation of the void space per unit volume of the column, which minimises the resistance to gas up-flow;
- minimisation of the friction, realised with an open shape in order to give good aerodynamic characteristics;
- minimisation of the costs, which rise with the weight per unit volume of the packing.

Sulzer MellapakPlus 452Y structured packing, manufactured in AISI 316, was chosen to be firstly qualified in TRIEX-II in order to minimise the risk of hold-up due to the high value of surface tension of the LiPb, as suggested by the manufacturer. The main design parameters are reported in Table 1.

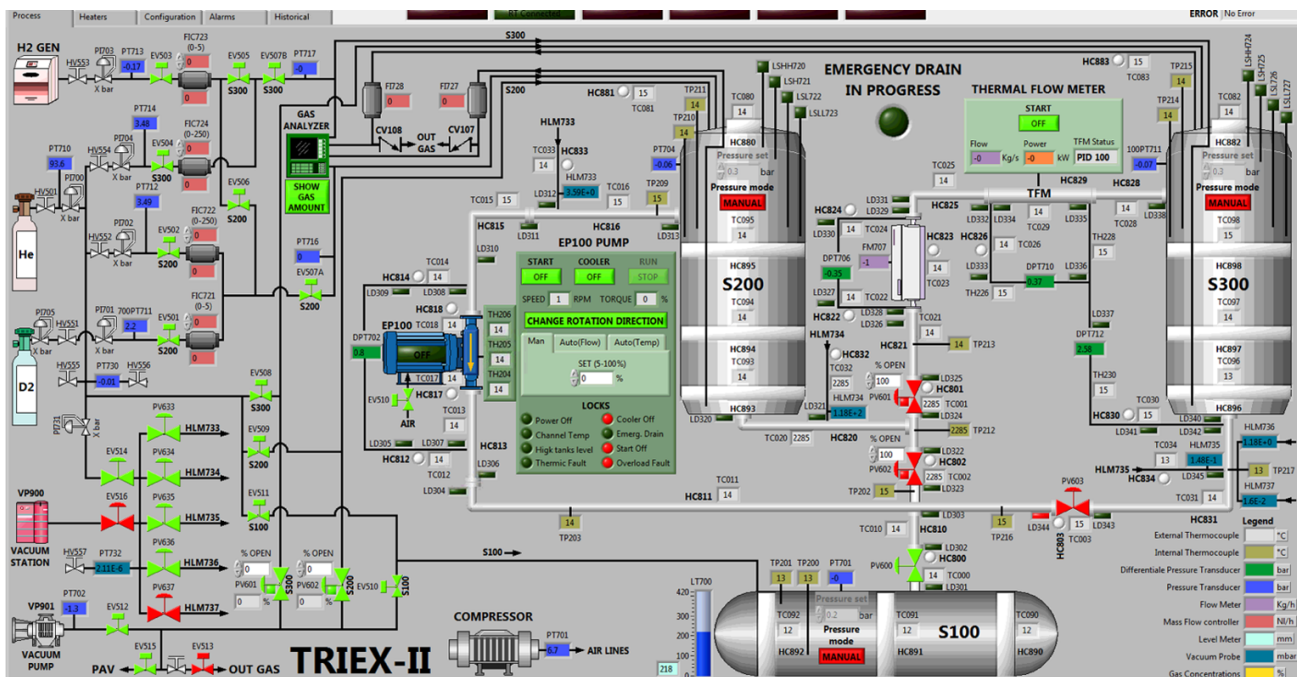


Figure 4: Main window of the DACS of TRIEX-II.

Table 1: Design parameters of the GLC mock-up equipped with MellapakPlus 452Y in TRIEX-II

Parameter	Value	Units
Design pressure	10	barg
Design temperature	530	°C
Max. operative temperature	500	°C
Voids	98	%
Surface-to-volume ratio	350	m ² m ⁻³
Design temperature	530	°C
Gas stripping flow rate range S300	50-450	Nl h ⁻¹
LiPb mass flow range in S300	0.2-4.5	kg s ⁻¹
Stripping gas for extractor S300	He, He+H ₂	
Material	2 1/4 Cr-1 Mo	
Column internal diameter	154.1	mm
Total height	2.5	m
Structured packing height	852	mm
Void fraction packing	95	%

The corrosion rate of the ferritic steel AISI 316 at 427 °C was evaluated by Chopra and Smith [18]. They found a corrosion rate equal to 82.1 $\mu\text{m y}^{-1}$ and a weight loss of 75 $\text{mg m}^{-2} \text{h}^{-1}$. This means that, in 5 years with continuous operation, $\sim 50\%$ of the filling material will be corroded by the LiPb. On the other hand, at a temperature of 371 °C, the corrosion rate would drop to 3.1 $\mu\text{m y}^{-1}$, leading to a corrosion of $\sim 1\%$ in 5 years. The operative temperature of TEU has, therefore, a remarkable impact on the behaviour

of the GLC unit. In the application for DEMO reactor the operative temperature foreseen is 330 °C therefore corrosion rate has not a relevant impact, instead for ITER application the working temperature is 450 °C but the lifetime of the components is shorter. Moreover, several solutions can be adopted in order to reduce the corrosion for this purpose: for instance, frequent substitutions of the material can be foreseen every 5 years, or structured packing realized in ferritic-martensitic steels with corrosion rates 10 times lower than ferritic ones [19] could be adopted. In TRIEX-II, the corrosion of the structured packing has no relevant effect on the extraction efficiency since the amount of impurities is negligible when compared to the total amount of LiPb. Moreover, impurities from the packing can precipitate in the channel of the PMP due to the effect of the magnetic field (magnetic traps) [20]. In order to reduce the corrosion rate and the amount of corrosion products generated by low corrosion steels as P22 is under evaluation for the filling materials.

In the extractor of TRIEX-II, the LiPb enters the upper part and it is uniformly distributed on the filling material by means of a dedicated diffuser. Due to the low solubility of hydrogen isotopes in LiPb and to its concentration gradient at the LiPb/gas interface, a mass transport occurs with the passage of hydrogen isotopes from the LiPb to the gas phase. The higher the LiPb/gas interface, the greater the total flow of extracted hydrogen isotopes. The extraction process of hydrogen isotopes from the LiPb is also determined

by the thickness of the LiPb film on the surface of the metal sheet that composes the packing of the column. The lower the LiPb film height, the lower the time required by hydrogen isotopes to diffuse from the LiPb to the LiPb/carrying gas interface.

The gas injection and extraction lines are normally kept at room temperature, but they are equipped with heating cables and thermal insulation. In this way, they can be heated in case LiPb enters in the lines and solidify. Then, once the loop is completely drained, LiPb can be removed by increasing the gas pressure in the lines.

5.2. Saturator (S200)

The saturator is a large vessel used to saturate hydrogen isotopes in LiPb by means of a mixed Gas-Liquid Contactor system, consisting of a combined bubble column and packed column [12] with a filling of AISI 316 structured material, of the same type of the extractor (Sulzer MellapakPlus 452Y). The hydrogen isotopes are injected together with helium working as carrier gas. After passing through the LiPb column, the outlet gas flow rate is monitored by means of a mass flow meter. The inlet and outlet gas lines of the saturator have been conceived, manufactured and equipped with the same approach used for the extractor.

5.3. Storage tank (S100)

The LiPb storage tank (Figure 5) is used for storing all the lithium-lead eutectic alloy contained in the circuit, including the one in the saturator, the extractor and the pipes, during the loading and draining phases of the system.

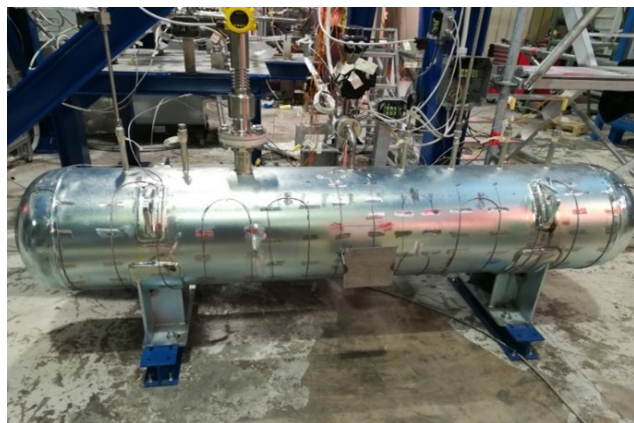


Figure 5: S100 storage tank equipped with thermocouples, relative pressure transducer, guided micro-wave level meter.

The eutectic LiPb was supplied by CAMEX in

the form of $30 \times 7.5 \times 7.5$ cm³ ingots, with a minimum certificated purity of 99.5% (99.96% nominal). The ingots are melted under vacuum in a dedicated furnace, shown in Figure 6 on the left, then the liquid metal is discharged by gravity through a filter in the storage tank. A total of 156 dm³ of LiPb is required to operate TRIEX-II, corresponding to 4 furnace loads.

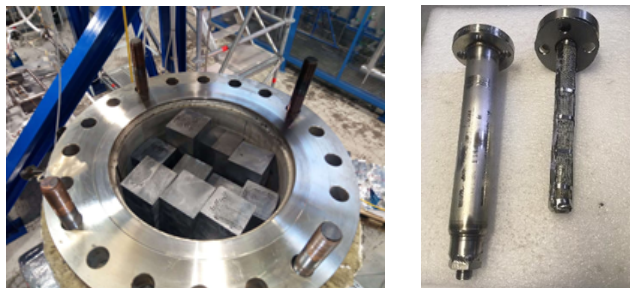


Figure 6: Melting furnace charged with LiPb ingots on the left and LiPb filter installed between melting tank and storage tank.

In order to verify the composition of the alloy after the loading phase, the eutectic point was checked analysing the temperature evolution during the cooling down to ambient temperature of the LiPb in the storage tank. During the phase change from liquid to solid, the heat removed from the LiPb does not influence its temperature, which remains constant. Fig. 4 shows the data measured by the three thermocouples of the storage tank. It is evident that the melting temperature is $T=235$ °C, confirming the eutectic point of the liquid metal alloy.

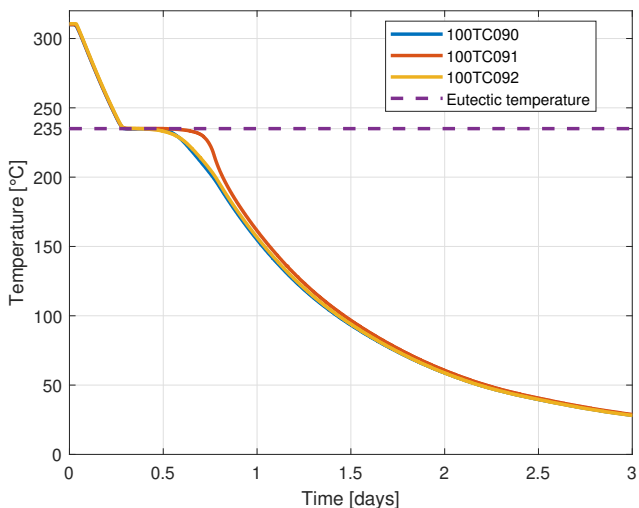


Figure 7: Temperature evolution during the cooling down of the LiPb in the storage tank measured by the thermocouples 100TC90, 100TC91 and 100 TC92.

5.4. Permanent magnets pump (EP100)

The LiPb flow in the circuit is guaranteed by a permanent magnets pump, whose operating principle is based on the magneto-hydro-dynamics (MHD) effect [21]. The pump, manufactured with Sm₂Co₁₇ magnets, must operate at a maximum operating temperature of 530 °C thanks to a proper cooling system with compressed air. The EP100 pump has two flanged 1 inch ASA 300 connections. The characteristic curve (Figure 8) of the pump was experimentally determined.

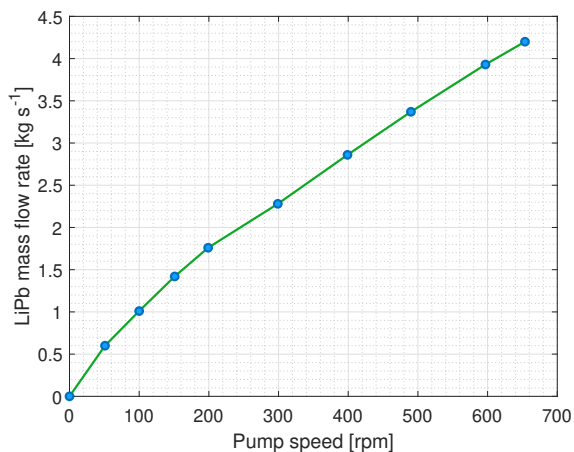


Figure 8: PMP pump characteristic curve.

6. Main instrumentation

The main instrumentation installed in TRIEX-II facility is described in the following paragraphs.

6.1. Hydrogen isotopes permeation sensors

Hydrogen isotopes are dissolved in LiPb at a given concentration c_H [mol m⁻³] and is in equilibrium with a partial pressure $p_{Q_2,eq}$ [Pa]. ENEA, in collaboration with Politecnico di Torino, developed sensors dedicated to the measurement of hydrogen isotopes partial pressure [22, 23]. These sensors are called permeation sensors as they are based on the physical principle of permeability of hydrogen through a membrane. Hydrogen permeation sensors (HPS) consist of a permeable helical-shaped component, immersed in the LiPb, and by a vacuum pressure transducer. TRIEX-II has three permeation sensors installed before the saturator (HLM733), after the saturator (HLM734) and after the extractor (HLM735). They are operated at medium vacuum (0.1-1 Pa) to ensure the correct pressure gradient in order to allow the permeation through the membrane. The operative range foreseen for this application is 10-1000 Pa. The helical

components and the pressure transducers are installed on the vacuum loop. Vacuum is pumped in the permeation sensors by a turbomolecular pump before the start of the experiments. The sensors (Figure 9) are made of α -iron (bcc), with a 99.5% purity, supplied by Goodfellow. The helical design allows to reduce the number of weldings, thus minimizing the problem of iron oxidation during the welding procedure and reducing the costs. The helical sensor is obtained by rounding a thin pipe around a cylindrical support. Only two welds are needed: a butt weld at the bottom of the pipe, in order to close it, and an orbital weld at the top, in order to connect the helix with a 1/8" Swagelok pipe (and thus to its pressure transducer). The current configuration derives from dedicated sensitivity analyses [23]. The Process Flow Diagram (PFD) of the whole sensor line is displayed in Figure 10.

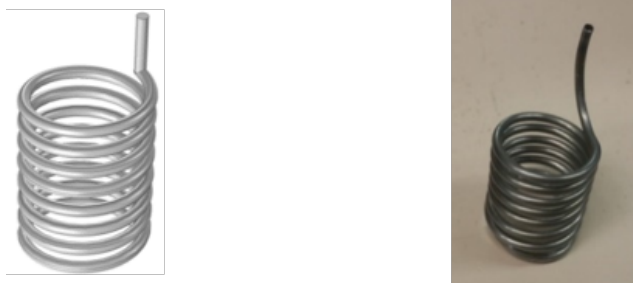


Figure 9: Helical sensor (drawing on the left, real helix on the right).

The sensors were calibrated in gas and liquid phase at 400°C and 450°C. The calibration at 450°C in liquid phase is shown in Figure 11. It is possible to observe that the three sensors achieved the equilibrium at the same partial pressure. The accuracy of the sensors is about 5% of the Full-Scale Output. The HPS are not able to discern between hydrogen and deuterium in the LiPb flow.

6.2. Quadrupole mass spectrometer

The quadrupole mass spectrometer is one of the most important components in the facility because it allows to measure the concentration of hydrogen or deuterium in helium stripping gas, thus allowing to close the mass balance of hydrogen isotopes. The quadrupole mass spectrometer is composed by an ion source, a mass filter (or quadrupole analyzer) and an ion detector. To work correctly, the vacuum chamber must be kept at about $5 \cdot 10^{-7}$ mbar.

Among different possible choices, the ESSCO GeneSys 200D gas analyzer was selected for TRIEX-II. One of the main advantages of this gas analyzer is that it is able to manage up to six inlets, thus

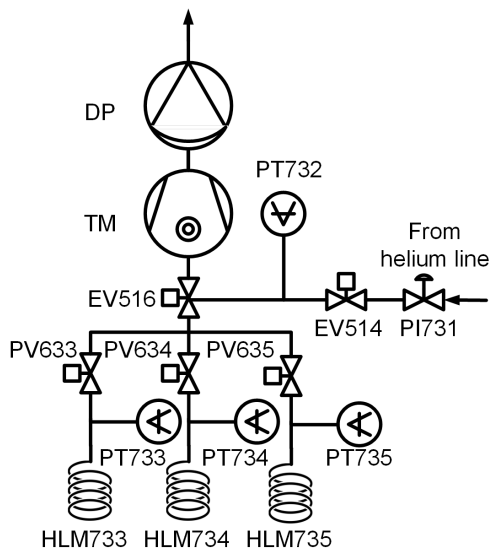


Figure 10: PFD of hydrogen permeation sensors line. HLM: hydrogen permeation sensor; PT: capacitive pressure transducer; PV, EV: electro-pneumatic valves; PI: pressure regulating valve; TM: turbomolecular pump; DP: diaphragm pump.

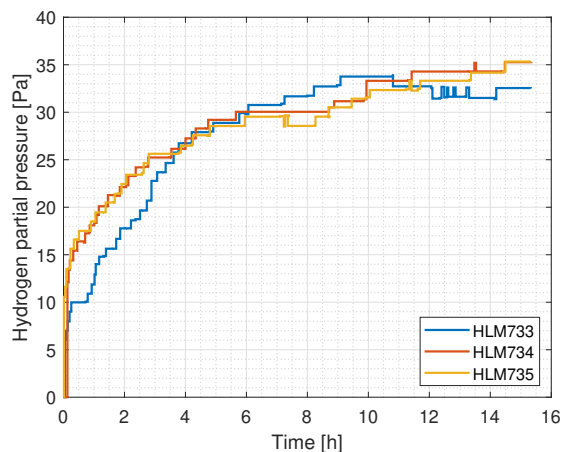


Figure 11: Permeation sensors pressure trend in flowing lithium-lead. LiPb mass flow rate 1 kg s^{-1} , operative temperature $450 \text{ }^\circ\text{C}$.

allowing to analyze the inlet and outlet gases of the saturator and of the extractor. Moreover, it allows to choose between two measuring ranges: 1-200 amu and 1-5 amu. The latter is used when it is necessary to discriminate the deuterium ($M_{D_2} = 4.0282 \text{ amu}$) and helium ($M_{He} = 4.0026 \text{ amu}$) peaks, allowing to measure the deuterium and the HD concentrations in the helium stripping gas. The Limit of Detection (LOD) is 1 ppb.

The gas analyzer has been tested in order to check the capability to distinguish chemical compounds

that have very similar molecular masses. The most important start-up procedure are the background and the calibration, that in TRIEX-II are performed with nitrogen and with a set of calibrated cylinders of He+H₂ and He+D₂. The hydrogen concentration in the calibrated cylinder is in the range expected for the experiments. Figure 12 shows that the system is able to distinguish helium from deuterium.

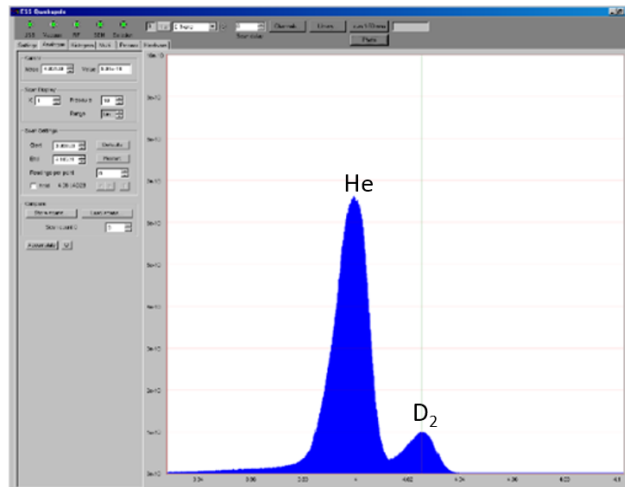


Figure 12: Acceptance test for EES GeneSys 200D: two distinct peaks for He and D₂ can be seen.

6.3. Thermal flow meter

A thermal mass flow meter used to measure LiPb mass flow is installed between the saturator and the extractor. This kind of instrument was designed by a joint collaboration between ENEA and Thermocoax, and it was characterized in IELLLO facility [14]. The thermal mass flow meter is a particular type of flow meter based on enthalpy balance, described by the following equation:

$$W_{hb} = \dot{m} \cdot c_p \cdot (T_{out} - T_{in}) \quad (1)$$

where W_{hb} [W] is the power supplied by a heating bulb, \dot{m} [kg s^{-1}] is the LiPb mass flow rate, c_p [$\text{J kg}^{-1} \text{K}^{-1}$] the LiPb specific heat, T_{out} [K] and T_{in} [K] are the temperatures measured by two PT100 sensors at the outlet and the inlet, respectively.

As displayed in Figure 13, the LiPb enters the instrument and its temperature is measured. Then, it is heated by the bulb, blended by the static mixer and finally its temperature is measured again. Two PT100 sensors are used to measure the temperature.

The instrument has a diameter of 2.5" and it is 800 mm long. All the parts of the instrument are made of AISI 316 or AISI 321 stainless steel. The instrument is designed to work at a maximum of 10 bar and $530 \text{ }^\circ\text{C}$. To protect the flow meter from the corrosion caused

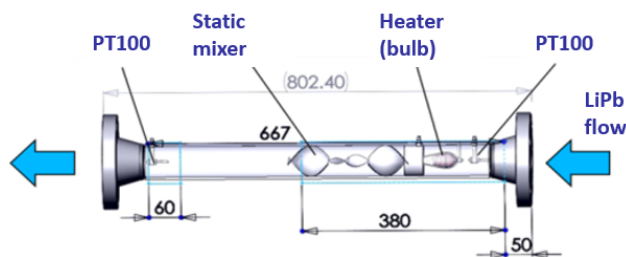


Figure 13: Sketch of the thermal mass flow meter.

by the LiPb flow, all the inner parts were coated by aluminizing process performed by Diffusion Alloys Ltd. The Al_2O_3 layer has a thickness of 75-125 μm .

The heating bulb has a maximum power of 6 kW, but it is usually operated at 2-3 kW so that the temperature of the LiPb is not remarkably increased. A dedicated Control system developed by ENEA allows to maximize the accuracy of the measure with the control of heating power supplied to the bulb. The measurement range is 0.5-5 kg s^{-1} .

6.4. Differential pressure transducers

Piezoresistive differential pressure transducers, supplied by Rosemount, measure the pressure difference in LiPb across the permanent magnet pump (range ± 20.7 bar), the thermal flow meter (range ± 2.5 bar) and the extractor (range ± 20.7 bar). The nominal accuracy of this instrument is 0.1% of the Full Scale Output. The installation procedure and the testing of this instrument is described in [14]. Each differential pressure transducer has two remote connectors that have to be installed at the two ends of the component whose pressure drops have to be measured. The remote connectors are filled with a particular silicone (1,3,5-trimethyl-1,1,3,5,5-pentaphenyl trisiloxane, $\text{C}_{33}\text{H}_{34}\text{O}_2\text{Si}_3$), intended for use in applications with high operating temperatures. The differential pressure transducer and mass flow meter allows to perform the fluid-dynamic characterisation of the main components installed in TRIEX-II.

7. Fluid-dynamics characterization: analysis of pressure drops

Concentrated and distributed pressure losses have been analytically evaluated [24]. The pressure drops related to the extractor and to the thermal mass flow meter were not included in the analytical calculation, as these have been measured by using differential pressure transducers. The saturator is not equipped with a differential pressure transducer because it is not a component that will be installed in the real LiPb loop of the WCLL TBS. Thus, its contribution to the

pressure drops is assumed to be equal to that of the extractor, being very similar in shape and dimensions.

The pressure drops measured across the thermal mass flow meter are practically negligible, in particular with low flow rates, as shown in Figure 14. The measured points were interpolated so that it was possible to find the correlation to calculate the pressure drops at the flow rates needed in the analytical evaluation. The error bars in this figure, and in the following ones, report the measuring error of the instrument, composed of the root-sum-square of the instrument accuracy and of the error in the signal acquisition chain.

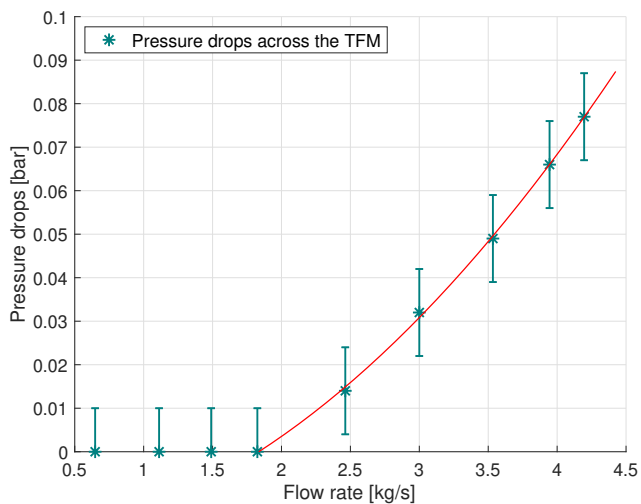


Figure 14: Pressure drops across the thermal flow meter.

The measurement of the pressure drops across the extractor was split in two parts, analyzing the variation of the pressure drops with LiPb mass flow rate (without any stripping gas flow rate, Figure 15) and with the stripping gas flow rate (at 1.2 kg s^{-1} , Figure 16). The figures show that the stripping gas has a higher impact than the LiPb mass flow rate on the pressure drops across the extractor.

The calculations of distributed and concentrated pressure drops were performed at different mass flow rates and the results (including the experimental value of the pressure drops of the extractor, saturator and thermal flow meter) are shown in Figure 17, where they are compared with the pressure drops measured by the differential pressure transducer installed across the permanent magnet pump. The average percentage difference between the two curves is about 33%. This difference is likely due to the fact that, in the analytical calculation, some details cannot be easily considered, such as all the penetrations of the instruments (e.g. thermocouples and helicoidal sensors).

Figure 18 shows the measured total pressure drops

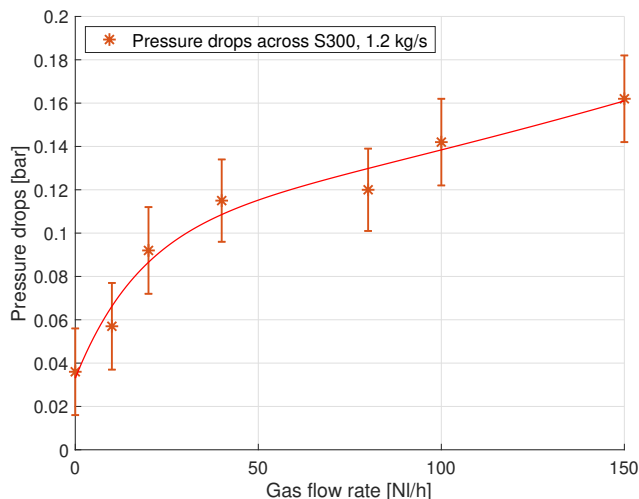


Figure 15: Pressure drops across the extractor at different stripping gas flow rate.

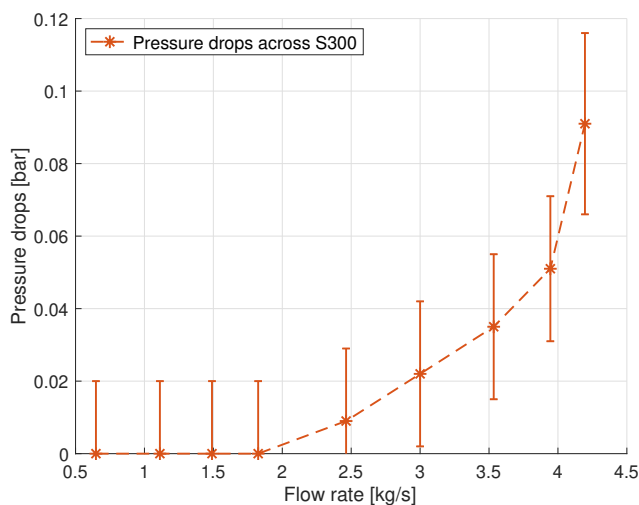


Figure 16: Pressure drops across the extractor at different LiPb mass flow rate.

compared with the contribution given by the extractor, which is quite small. This result is encouraging for the LiPb loop of the WCLL TBS, as the tested mock-up has relevant dimensions considering the operative conditions.

8. Methods to evaluate the extraction efficiency

The calculation of the extraction efficiency of the GLC mock-up of TRIEX-II can be experimentally evaluated in two ways:

- (i) Evaluation by means of hydrogen permeation sensors;
- (ii) Evaluation by means of mass spectrometry.

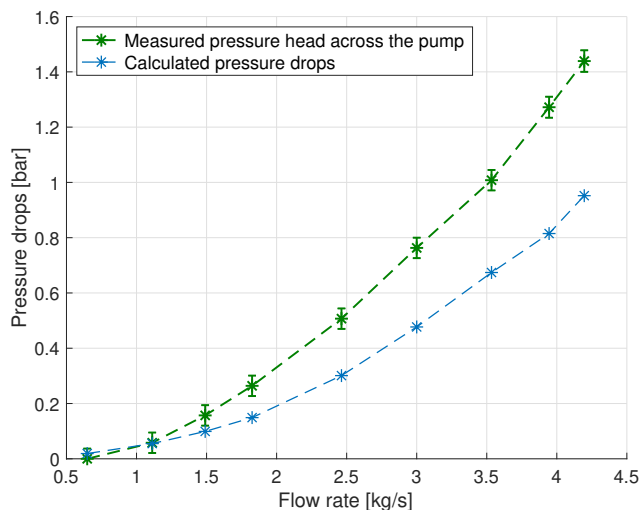


Figure 17: Experimental vs calculated pressure drops (with experimental values for the extractor, the saturator and the thermal flow meter).

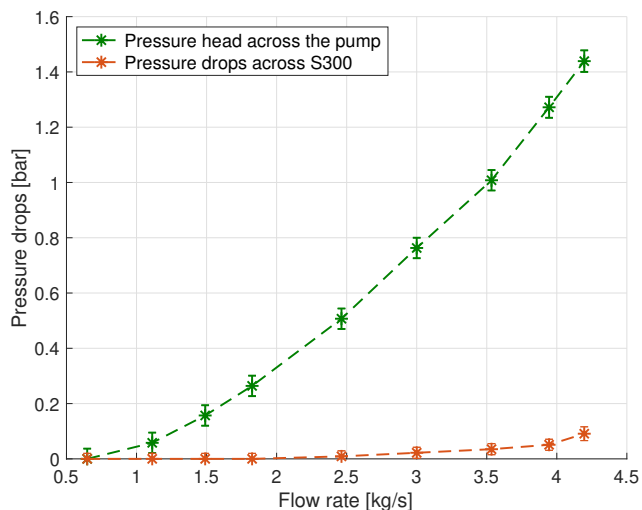


Figure 18: Measured pressure drops as a function of mass flow rate.

In particular, the second method requires to know the Sieverts' constant. In literature, several experiments were performed to determine the hydrogen solubility in LiPb, giving different results. Sieverts' constants by Aiello [25], Reiter [26] and Chan-Veleckis [27] are the most used for the experimental campaigns and for numerical codes. Nevertheless, the three correlations give different values of the constant due different experimental methods adopted. While the Sieverts' constant by Aiello was found using the absorption technique, Reiter used a method based on pressure increase measurements in a known volume during unloading of a sample (desorption technique), which was previously loaded. Instead, Chan and Veleckis used a thermodynamic model to evaluate

the Sieverts' constant. According to Reiter, the method used in determining the constant influences the experimental results. Vacuum, wall and container contributions are other parameters that can affect the results. Also Aiello confirms that the solubility values found in their experiments are in the range obtained by other authors using the same technique.

In the following, the two methods to evaluate the extraction efficiency are described. Figure 19 shows a sketch of the mass balance through the extractor, where also the nomenclature used in the following paragraphs is illustrated.

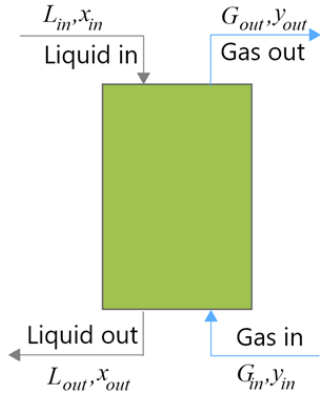


Figure 19: Sketch of the extractor with the nomenclature of the efficiency calculations.

8.1. Evaluation by means of partial pressures of hydrogen isotopes in LiPb

The basic definition of extraction efficiency is used to calculate the extraction efficiency through permeation sensors:

$$\eta = \frac{c_{in} - c_{out}}{c_{in}} = 1 - \frac{c_{out}}{c_{in}} \quad (2)$$

where c_{in} [mol m⁻³] is the concentration of hydrogen isotopes at the inlet of the extractor and c_{out} [mol m⁻³] is the concentration of hydrogen isotopes at the outlet of the extractor. The Sieverts' law allows to evaluate the solubility of hydrogen isotopes in LiPb knowing their partial pressure ($p_{H_2,eq}$) when the thermodynamic equilibrium is reached:

$$c_H = k_S \sqrt{p_{H_2,eq}} \quad (3)$$

Introducing the Sieverts' law into Equation 2:

$$\eta = 1 - \frac{k_S \sqrt{p_{out,eq}}}{k_S \sqrt{p_{in,eq}}} = 1 - \sqrt{\frac{p_{out,eq}}{p_{in,eq}}} \quad (4)$$

where $p_{in,eq}$ [Pa] (measured by the HPS at the inlet of the extractor) and $p_{out,eq}$ [Pa] (measured by the HPS at the outlet of the extractor) are the partial pressures of hydrogen isotopes at the inlet and at

the outlet of the extractor in equilibrium conditions, respectively. In this way, the efficiency is only function of the pressure measured by the permeation sensors at the inlet and at the outlet of the extractor and it is independent of the value of the Sieverts' constant.

The accuracy of this method is linked with the accuracy of the two permeation sensors (HLM 734 and HLM 735). The pressure trend of the pressure sensors must be stable in order to perform this measure. It should be observed that this method is valid for each technology to be tested in TRIEX-II.

8.2. Evaluation by means of mass spectrometry

The efficiency can be also expressed in terms of ratio of molar fractions:

$$\eta = \frac{x_{in} - x_{out}}{x_{in}} = 1 - \frac{x_{out}}{x_{in}} \quad (5)$$

where x_{in} and x_{out} [-] are the molar fractions of the hydrogen isotopes in the LiPb at the inlet and outlet of the extractor, respectively. The difference between x_{in} and x_{out} can be written with a mass balance in the column:

$$L(x_{in} - x_{out}) = 2G(y_{out} - y_{in}) \quad (6)$$

where L and G [mol s⁻¹] are the molar liquid metal and gas flow rates, y_{in} [-] and y_{out} [-] are the molar fraction of the hydrogen isotopes in the stripping gas at the inlet and outlet of the extractor, and the factor 2 takes into account the fact that in the eutectic alloy the hydrogen exists in atomic form, while in helium it has recombined in the molecular form H₂/D₂/HD. This equation is simply an integration of the hydrogen molar balance at a generic height of a counter-current extraction column [15]. The inlet molar fraction can be calculated as:

$$x_{in} = k_S \sqrt{p_{in,eq}} \frac{M_{LiPb}}{\rho_{LiPb}} \quad (7)$$

where k_s [mol m⁻³ Pa^{-0.5}] is the Sieverts' constant, M_{LiPb} [kg mol⁻¹] is the molecular weight of the LiPb and ρ_{LiPb} [kg m⁻³] is the LiPb density. From Equation 6 and Equation 7, the efficiency becomes:

$$\eta = \frac{2\rho_{LiPb}}{k_S \sqrt{p_{in,eq}} M_{LiPb}} \frac{y_{out} - y_{in}}{L/G} \quad (8)$$

In this case, it is possible to determine the GLC efficiency measuring the stripping gas inlet/outlet composition and the partial pressure in LiPb. The analysis of the efficiency calculated with the Sieverts' constant measured by Aiello and Reiter can supply additional information related the reliability of these values.

9. Preliminary results obtained

A preliminary characterisation of GLC was carried out with 0.5 vol. % hydrogen in the helium stripping gas and deuterium saturated in the LiPb. The GLC performance was investigated to simulate the nominal operative conditions of the TBM LiPb loop at 450 °C, liquid metal mass flow rate in the range 0.2-0.6 kg s⁻¹ and stripping gas flow rate in the range 50-100 Nl h⁻¹. The efficiency was measured by the support of hydrogen isotopes permeation sensors, that allow to measure the initial deuterium concentration in the liquid metal and the mass spectrometer system used to measure the tritium extraction flux (HD plus D₂). The D₂ partial pressure is 139 Pa. Assuming equal solubility of hydrogen isotopes (hydrogen, deuterium and tritium) in LiPb, the Sieverts' constants are related to each other by means of the following relationship [28, 29]:

$$k_{S,D}\sqrt{p_{D_2}} = k_{S,H}\sqrt{p_{H_2}} \quad (9)$$

where $p_{D_2}/p_{H_2} = \sqrt{2}$. Hence, it follows that:

$$k_{S,D} = k_{S,H} \cdot 2^{-1/4} \quad (10)$$

This means that the Sieverts' constant of deuterium is about 84% the one for hydrogen, i.e. less deuterium is solubilized in the bulk of the liquid metal.

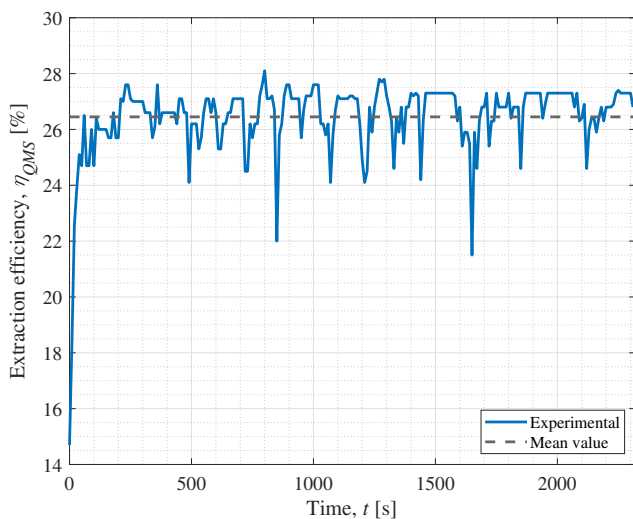


Figure 20: Extraction efficiency for test at 450 °C, $L = 0.6 \text{ kg s}^{-1}$, $G = 100 \text{ Nl h}^{-1}$.

Figure 20 shows the extraction efficiency measured by mass spectrometer. The measure was repeated three times in order to confirm the results obtained. An average extraction efficiency of 26%, calculated with Equation 8, is obtained, assuming Aiello's correlation for Sieverts' constant. The L/G ratio is equal to 4.4 l_{LiPb} Nl_{He+H₂}⁻¹. It should be noted that currently only the measurement of efficiency using the ESS GeneSys

200D quadrupole mass spectrometer is possible for tests with different hydrogen isotopes, since HPS cannot distinguish them from each other. In the future, the HPS will be equipped with dedicated mass spectrometers to allow discrimination between different hydrogen isotopes. The effect of HT recombination on tritium extraction efficiency was evaluated more relevant reducing the liquid metal mass flow rate up to 0.2 kg s⁻¹ and the stripping gas flow reaching value of efficiency up to 44%, Figure 21, which corresponds to an L/G ratio of 1.4 l_{LiPb} Nl_{He+H₂}⁻¹. Additional tests will be completed in the frame of EUROfusion FP9 project in order to confirm the analyses performed.

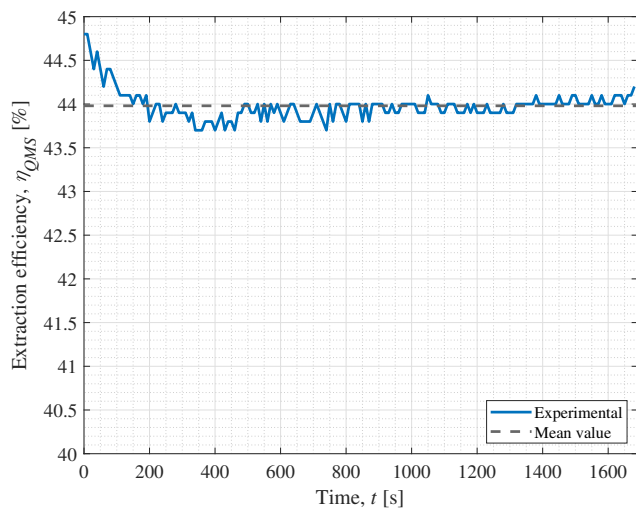


Figure 21: Extraction efficiency for test at 450 °C, $L = 0.2 \text{ kg s}^{-1}$, $G = 52 \text{ Nl h}^{-1}$.

10. Conclusions and future work

In the present work, a new facility, named TRIEX-II and installed at ENEA Brasimone research centre, was presented. The facility was designed with the aim of characterizing the extraction technologies for the TEU of ITER and DEMO based on the WCLL concept. The main systems constituting the facility are the lithium-lead loop, the vacuum system, the gas loop and the compressed air circuit. Regarding the lithium-lead loop, it is constituted by the storage tank, the saturator, the extractor and the permanent magnets pump.

The storage tank is used for storing all the lithium-lead eutectic alloy contained in the circuit. The LiPb, with a minimum certified purity of 99.5%, was melted in a dedicated furnace for a total of 156 dm³. The eutectic composition was verified during a cooling down procedure to ambient temperature. The saturator is based on the principle of bubble columns but presents also a structured Sulzer MellapakPlus

452Y filling material. The mock-up to be qualified in the present asset is the packed column, belonging to the family of Gas-Liquid Contactor technologies, where a gas and liquid phase are brought into contact allowing a diffusion interchange between them. The extractor mock-up is equipped with the MellapakPlus 452Y structured packing.

Most of the instrumentation present in TRIEX-II was specifically designed and manufactured for the operation in LiPb at high temperature. Within this frame, special emphasis should be put on the hydrogen permeation sensors, developed in collaboration with Politecnico di Torino, and on the thermal flow meter, developed by a joint collaboration between ENEA and Thermocoax. Hydrogen permeation sensors are helical-shaped pure α -iron sensors for the measurement of hydrogen isotopes concentration in LiPb. They are placed, before the saturator, after the saturator and after the extractor. Their calibration was performed both in liquid and gas phase. On the other hand, the thermal flow meter, installed between the saturator and the extractor, was previously characterized in the lithium lead facility IELLLO. Finally, to cover the operative conditions foreseen in ITER and DEMO reactors, TRIEX-II was equipped with a quadrupole mass spectrometer able to measure concentrations in the stripping gas up to 1 ppb. Its capability to manage up to six inlets allows to analyse the inlet and outlet gases coming from both the saturator and the extractor.

From the fluid-dynamic characterization point of view, concentrated and distributed pressure drops were evaluated. The pressure drops related to the extractor and to the thermal mass flow meter were measured by means of differential pressure transducers. Concerning the extractor, the analysis was performed by considering the pressure drops with LiPb mass flow rate and with the stripping gas mass flow rate, resulting in a higher impact of the latter with respect to the former. The calculation of the distributed and concentrated pressure drops was performed at different mass flow rates and compared to the experimental results.

The efficiency calculation of the GLC mock-up was presented according to two different methods. The first method is a general one and can be applied to the different technologies to be tested in TRIEX-II. In particular, it is based on the efficiency definition considering the partial pressure measured by the hydrogen permeation sensors. In this way, it is possible to obtain a value which is independent of the Sieverts' constant of hydrogen isotopes solubilized in the LiPb. The second method is based on a mass balance on the GLC mock-up and relates the extraction efficiency to the concentrations measured by the quadrupole mass

spectrometer. In this way, however, the correlation depends upon the Sieverts' constant. This last method can be used to have a comparison between the efficiency measured by the hydrogen permeation sensor and the efficiency measured by the quadrupole mass spectrometer.

Lastly, a preliminary efficiency measurement of the GLC mock-up installed in TRIEX-II was presented. Both tests were conducted solubilizing deuterium in the LiPb and using a mixture of helium plus hydrogen as stripping gas. The first test showed an efficiency of 26% for $L/G = 4.4 \text{ l}_{\text{LiPb}} \text{ Nl}_{\text{He+H}_2}^{-1}$, which was increased to 44% by reducing the L/G ratio to $1.4 \text{ l}_{\text{LiPb}} \text{ Nl}_{\text{He+H}_2}^{-1}$. Future research will be focused on the prosecution of the experimental characterization of the GLC and the characterization of the PAV mock-up in the range of operation foreseen for the WCLL TBS and WCLL BB.

Acknowledgements

This work has been carried out within the framework of the EUROfusion Consortium and has received funding from the Euratom research and training programme 2014-2018 and 2019-2020 under grant agreement No 633053. This work has been also funded by Fusion for Energy under the contract F4E-FPA-372-SG04. The views and opinions expressed herein do not necessarily reflect those of the European Commission.

References

- [1] Aubert J, Aiello G, Alonso D, Batal T, Boullon R, Burles S, Cantone B, Cismondi F, Nevo A D, Maqueda L, Morin A, Rodríguez E, Rueda F, Soldaini M and Vallory J 2020 *Fusion Engineering and Design* **160** 111921
- [2] Del Nevo A, Arena P, Caruso G, Chiovaro P, Di Maio P, Eboli M, Edemetti F, Forgione N, Forte R, Froio A, Giannetti F, Di Gironimo G, Jiang K, Liu S, Moro F, Mozzillo R, Savoldi L, Tarallo A, Tarantino M, Tassone A, Utili M, Villari R, Zanino R and Martelli E 2019 *Fusion Engineering and Design* **146** 1805–1809
- [3] Federici G, Boccaccini L, Cismondi F, Gasparotto M, Poitevin Y and Ricipito I 2019 *Fusion Engineering and Design* **141** 30–42
- [4] Demange D, Antunes R, Borisevich O, Frances L, Rapisarda D, Santucci A and Utili M 2016 *Fusion Engineering and Design* **109-111** 912–916
- [5] Utili M, Tincani A, Candido L, Savoldi L, Zanino R, Zucchetti M, Martelli D and Venturini A 2019 *IEEE Transactions on Plasma Science* **47** 1464–1471
- [6] Cismondi F, Spagnuolo G, Boccaccini L, Chiovaro P, Ciattaglia S, Cristescu I, Day C, Del Nevo A, Di Maio P, Federici G, Hernandez F, Moreno C, Moscato I, Pereslavitsev P, Rapisarda D, Santucci A and Utili M 2020 *Fusion Engineering and Design* **157** 111640
- [7] Hernández F, Pereslavitsev P, Kang Q, Norajitra P, Kiss B, Nádasi G and Bitz O 2017 *Fusion Engineering and Design* **124** 882–886
- [8] Papa F, Utili M, Venturini A, Caruso G, Savoldi L, Bonifetto R, Valerio D, Allio A, Collaku A and Tarantino M 2021 *Fusion Engineering and Design* **166** 112313

- [9] Okino F, Yagi J, Tanaka T, Sagara A and Konishi S 2019 *Fusion Engineering and Design* **146** 898–901
- [10] Ricapito I, Aiello A, Bükki-Deme A, Galabert J, Moreno C, Poitevin Y, Radloff D, Rueda A, Tincani A and Utili M 2018 *Fusion Engineering and Design* **136** 128–134
- [11] Aiello A, Ciampichetti A, Utili M and Benamati G 2007 *Fusion Engineering and Design* **82** 2294–2302
- [12] Utili M, Aiello A, Laffi L, Malavasi A and Ricapito I 2016 *Fusion Engineering and Design* **109-111** 1–6
- [13] Anderson T L 1980 *Evaluation of the corrosion resistance of 2 1/4 Cr-1 Mo steel in a lithium-lead liquid* Master's thesis Colorado School of Mines
- [14] Venturini A, Papa F, Utili M and Forgione N 2020 *Fusion Engineering and Design* **156** 111683
- [15] Green D W and Perry R H 2008 Equipment for distillation, gas absorption, phase dispersion and phase separation *Perry's Chemical Engineers Handbook* (New York, New York, USA: McGraw-Hill)
- [16] Alpy N, Dufrenoy T and Terlain A 1998 *Fusion Engineering and Design* **39-40** 787–792
- [17] Alpy N, Terlain A and Lorentz V 2000 *Fusion Engineering and Design* **49-50** 775–780
- [18] Chopra O and Smith D 1986 *Journal of Nuclear Materials* **141-143** 566–570
- [19] Utili M, Bassini S, Tarantino M and Martelli D 2018 Current knowledge on compatibility of reduced activation ferritic-martensitic steels in PbLi. Workshop on liquid metal technology: materials issues in fusion, fission and solar energy applications, Madrid, Spain URL http://www.h2020-m4f.eu/filesharer/documents/Workshops/Liquid_Metal_Workshop/Presentations/
- [20] Tortorelli P and Chopra O 1981 *Journal of Nuclear Materials* **103** 621–632
- [21] Candido L, Alberghi C, Papa F, Ricapito I, Utili M, Venturini A and Zucchetti M 2021 *Fusion Science and Technology*
- [22] Ciampichetti A, Zucchetti M, Ricapito I, Utili M, Aiello A and Benamati G 2007 *Journal of Nuclear Materials* **367-370** 1090–1095
- [23] Candido L, Utili M, Zucchetti M, Ciampichetti A and Calderoni P 2017 *Fusion Engineering and Design* **124** 735–739
- [24] Idelchik I 2000 *Handbook Of Hydraulic Resistance* 3rd ed (Mumbai, India: Jaico Publishing House)
- [25] Aiello A, Ciampichetti A and Benamati G 2006 *Fusion Engineering and Design* **81** 639–644
- [26] Reiter F 1991 *Fusion Engineering and Design* **14** 207–211
- [27] Chan Y and Veleckis E 1984 *Journal of Nuclear Materials* **123** 935–940
- [28] Veleckis E, Yonco R and Maroni V 1977 *Journal of the Less Common Metals* **55** 85–92
- [29] Candido L, Alberghi C and Utili M 2021 *Vacuum* **191** 110414